DEVELOPMENT OF A HIGH PERFORMANCE MICROVIBRATION ISOLATION SYSTEM

Emilia Wegrzyn [(1)], Alessandro Stabile [(1)], Guglielmo S. Aglietti [(1)], Guy Richardson [(2)] , Peter Spanoudakis[(3)], Florent Cosandier [(3)], Philippe Schwab [(3)], Geert Smet [(4)]

[(1)] Surrey Space Centre University of Surrey, Guildford, GU2 7XH, UK; EMail: a.stabile@surrey.ac.uk

[(2)] Surrey Satellite Technology Ltd. (SSTL) 20 Stephenson Rd, Surrey Research Park, Guildford, GU2 7YE, UK

[(3)] Centre Suisse d'Electronique et de Microtechnique (CSEM), Rue Jaquet-Droz 1, 2002 Neuchâtel, Switzerland

[(4)] ESA/ESTEC Keplerlaan 1, PO Box 299, 2200 AG, Noordwijk, Netherlands

ABSTRACT

This paper presents the current status of a novel hexapod platform capable of providing high microvibration attenuation performance both at low and high frequency, while maintaining a system architecture that is relatively simple (e.g. no control algorithm, only flexure-based joints, cross-coupling between transferred forces and moments to be almost eliminated). This work shows the assembly of a first full-model breadboard and the good correlation between simulations and test results under microvibration loads.

INTRODUCTION

Hexapod platforms are a type of parallel manipulator that have been studied and developed extensively in the last 50 years due to the several advantages they present especially for applications requiring high load carrying capacity and precise positioning [1,2]. Parallel manipulators are capable of carrying great loads because the total load is shared among all the parallel links. The hexapod platform became popular in the 60s when three research groups came up with three designs that were fairly similar [3-5]. In particular, the most common hexapod platform is made of six variable-length struts that are arranged in a way to provide motions in six Degrees of Freedom (DoF) by using universal and spherical joints and adopting the cubic configuration. These platforms are not only used regularly for terrestrial applications [6-8] but they have also been identified as possible solutions for space missions requiring challenging optical stability on board a spacecraft. Examples of hexapod platforms for space missions are VISS (Vibration Isolation and Suppression System which had six passive viscous dampers [9]) and SUTE (Satellite Ultraquiet Isolation Technology Experiment made of six active struts with embedded piezoelectric actuators [10]). Nevertheless, these mechanisms are rarely integrated on satellites due to some limitations and drawbacks that they still present such as dynamic complexity, considerable amount of added mass, and need for control algorithm and sensors [11]. All these aspects, together with the limited isolation performance enhancement, have severely affected the use of hexapod platforms for high-sensitivity missions. For these reasons, extensive research has been carried out on one hand to investigate alternative damping methods to be embedded within the strut elements so to enhance the isolation performance, and on the other hand to improve the system dynamics which could be highly affected by improper boundary conditions or rattling effects within the joints.

Following these considerations, a team made by SSC, SSTL and CSEM has been working for over 2 years on the design of a novel hexapod platform capable of providing high micro-vibration attenuation performance both at low and high frequency, while maintaining a system architecture that is relatively simple (e.g. no control algorithm, only flexure-based joints, cross-coupling between transferred forces and moments to be almost eliminated). In terms of damping method, the team has chosen to use Electromagnetic Shunt Dampers (EMSD), which is a technology developed by SSC and SSTL over the last 5 years [12-15]. In particular, with the use of a negative-resistance converter, EMSDs have been proved to operate as semi-active dampers capable of combining the advantages of passive dampers (roll-off slope of -40 dB/decade) and active dampers (elimination of the resonance peak) without requiring either an active control algorithm or high input power.

This paper describes the current status of the developed hexapod platform, the performance analysis and the correlation with the test results. The highlights of the test results carried out on the single struts and on the fully assembled hexapod are presented in the paper together with the lessons learned from the testing of such a complex system.

PERFORMANCE ANALYSIS

A 3D representation of the Simulink model can be seen in Figure 1 and Figure 2. In the model, the hexapod is mounted on top of a triangular dynamometric table (A.K.A. Kistler table). It is noted that for simplicity, the mass and inertia of the payload (in this case a cluster of four reaction wheels and the triangular brackets that supports them) are lumped in the sphere shown on the top of the bipods in Figure 1. In this paper, the main focus is on two Transfer Functions (TF), TF11 (which is also equal to TF22) and TF33. The former is the TF associated with the input force and the measured output

force along the X axis, whereas the latter is the same but for the Z axis. As it can be seen in Figure 3, the TF11 and TF33 show the slope of -80 dB/dec between 30 and 100Hz, until they start to go up due to the bending modes of the struts. These modes are originated by the fact that the flexures within the struts although having high lateral stiffness it is still not infinite. Even though these modes compromise the attenuation at high frequency (e.g. above 150 Hz in this example), it is important to notice that such modes are only related to the strut design itself and they are independent from the mass supported on top of the hexapod. In other words, this issue now becomes a design exercise at subsystem level aimed at pushing the bending modes of the struts above 500Hz without affecting the low frequency performance. The project team will work on updating the strut design through a twofold approach, which is on one side to increase the lateral stiffness provided by the flexure, but on the other hand to further decrease the inertia of the strut as well, especially of the moving parts.

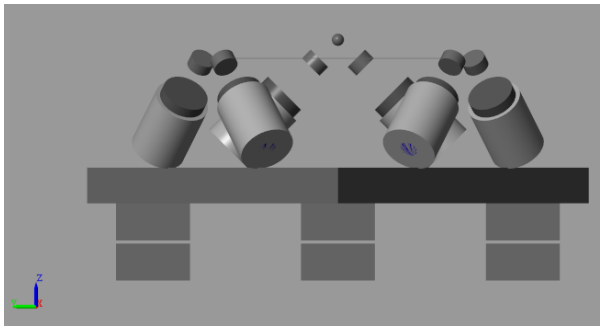

Figure 1. Simulink model of the fully assembled hexapod placed on top of a triangular dynamometric table (A.K.A. Kistler table). Front view.

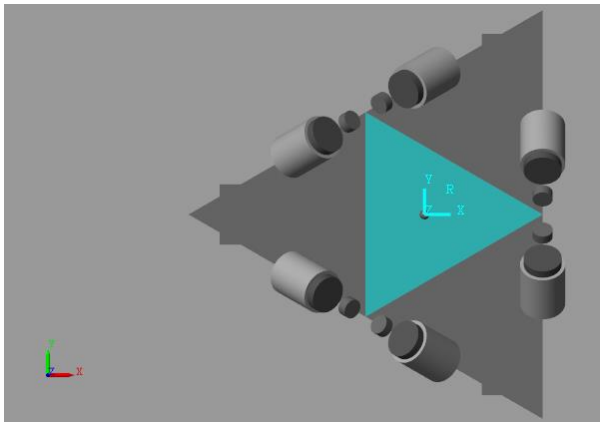

Figure 2. Simulink model of the fully assembled hexapod placed on top of a triangular dynamometric table. Top view.

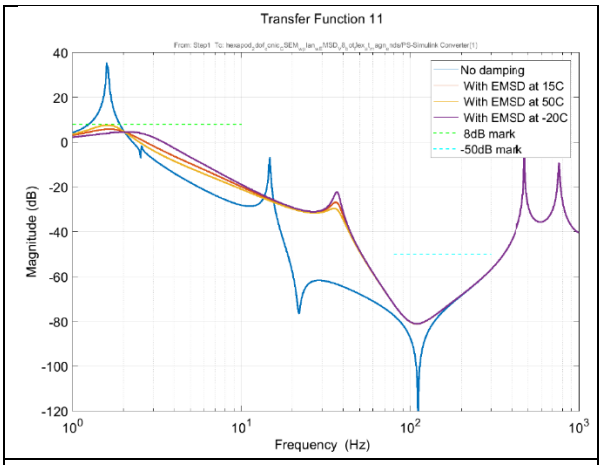

(a)

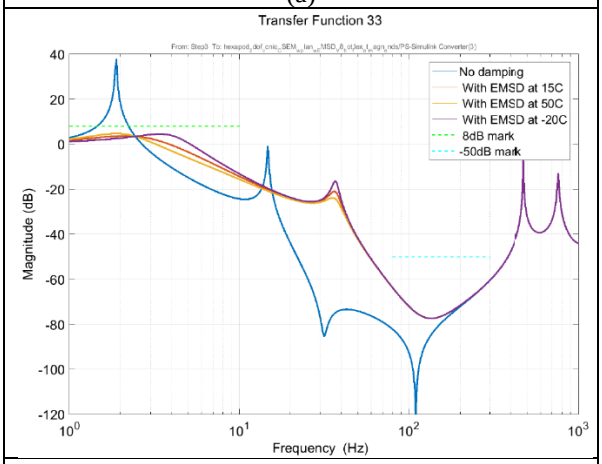

(b)

Figure 3. Example of two force transfer functions, TF11 (input and output along X) and TF33 (input and output along Z). Both plots show the case without damping (blue curve) compared with the cases with damping and at different temperature conditions.

TEST RIG DESIGN

The design of the test rig required intense effort from the project team in order to achieve a rig which minimizes its interference with the recorded forces and accelerations. In particular, the main focus was to reduce the environmental noise picked up by the sensors, reduce the effect of the offloading system (e.g. bungee cords) as well as removing secondary modes within the dynamometric table. Nonetheless, due to the challenging nature of this set up it was difficult to overcome all the challenges and some of the limitations in the test results will be explained in the next sections. The test rig can be seen in Figure 4. The top platform is characterized by a mass of about 30kg obtained with the triangular bracket and four dummy reaction wheels (each with a mass of about 5kg).

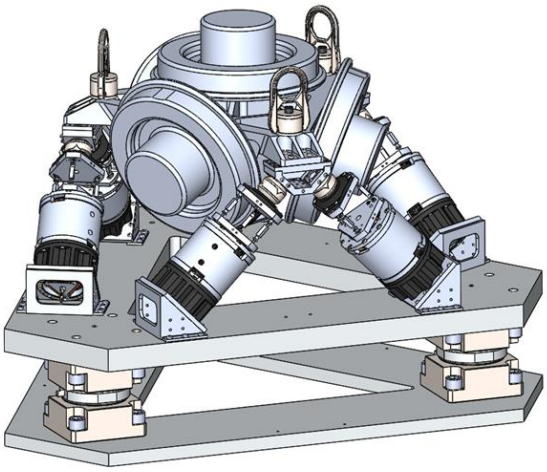

Figure 4. CAD model of the fully assembled hexapod with four dummy reaction wheels mounted on top.

TEST CAMPAIGN ON INDIVIDUAL STRUTS

Each individual strut was tested separately to characterize its performance to a longitudinal input. The test setup for each strut can be seen in Figure 5. The TF33 for the case without damping (ND) and the one with the EMSDs ON (WD) can be seen respectively in Figure 6 and Figure 7. For both figures, the comparison with the Simulink simulation is shown after the model parameters were tweaked to match the measured ones (e.g. parameters like the supported mass, the coil resistance and the flexure stiffness). The comparison between the test results and the simulations shows good correlation for the first two peaks and for the trend up to 100Hz. After that, the test results show the strut bending modes. It is noted that the Simulink simulations do not show such modes because in an ideal case (as it is in Simulink) such bending modes would not be excited by a vertical input. However, in a real case scenario, even a small offset or an angle of the mini-shaker would cause the excitation of those modes.

From the Simulink model for a single strut, it was expected to have the first bending mode at about 250Hz, but the test results suggested that the struts have lower bending stiffness than expected. An investigation was carried out with Nastran finite element analysis and it was concluded that in order to have bending modes as shown in Figure 6 and Figure 7 the bending stiffness (generated mostly by the lateral stiffness of the membrane guides and the parts clamping them) needs to be almost one third of the expected one (Figure 8 shows the bending modes obtained through Nastran). This aspect was further investigated, and an update of the strut design will be made following the lessons learned from this test campaign.

Nevertheless, the similarity between all the struts gave the project team confidence in proceeding with the hexapod testing as the main goal of this first test campaign is to generate a well, correlated Simulink model.

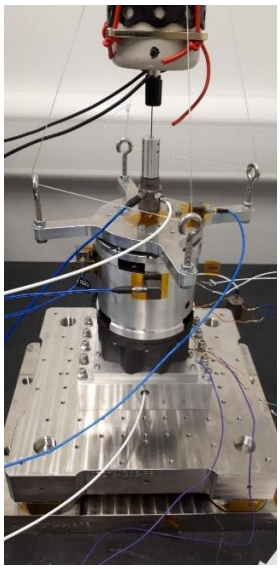

Figure 5. Test setup for the performance evaluation of each individual strut. Input force inject by mini-shaker and along the Z axis.

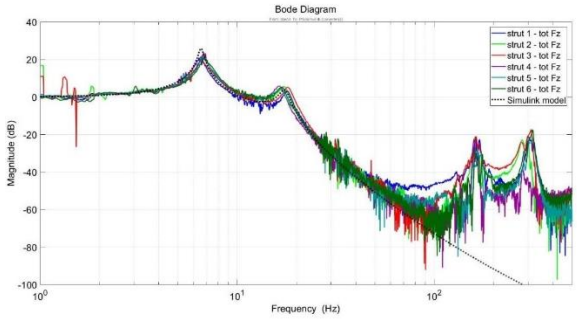

Figure 6. Vertical TF for each of the six struts with no damping (ND) conditions. Their TFs are then compared with the Simulink analytical model

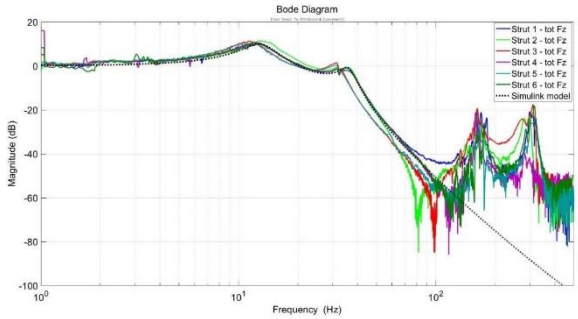

Figure 7. Vertical TF for each of the six struts with damping (WD) conditions. Their TFs are then compared with the Simulink analytical model

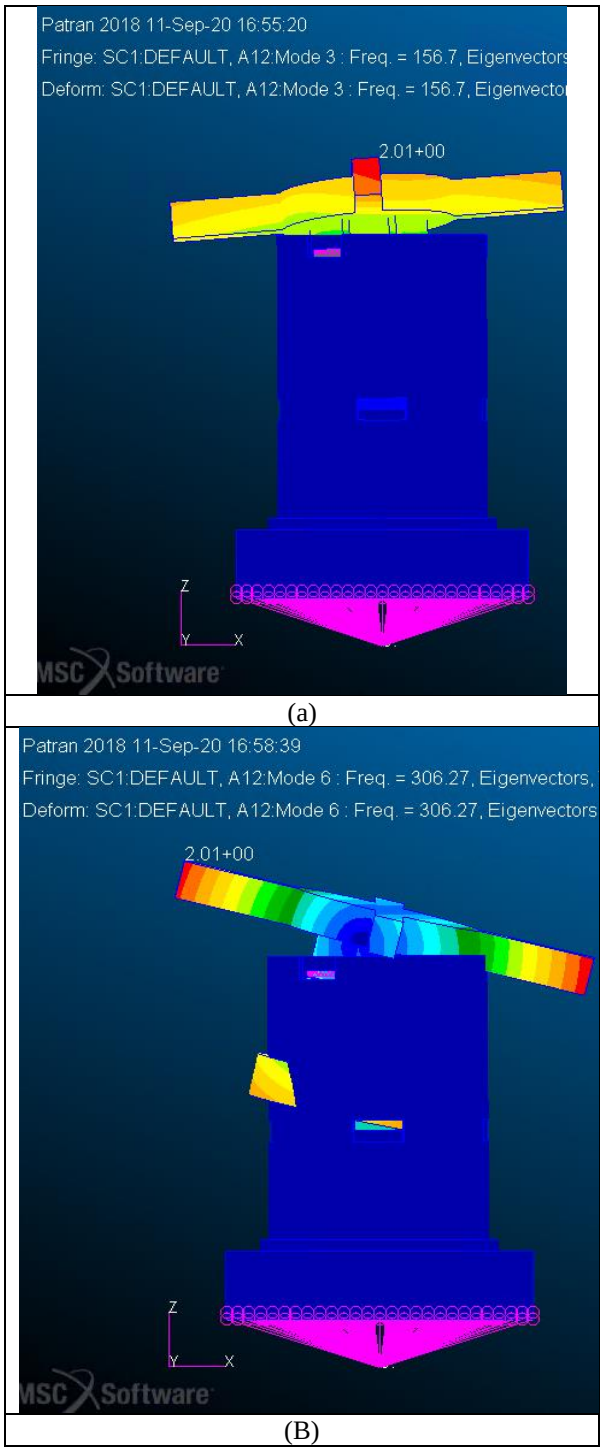

Figure 8. Bending modes of single struts obtained with Nastran FEA

TEST CAMPAIGN ON FULLY ASSEMBLED HEXAPOD

The fully assembled hexapod mounted on top of the triangular dynamometric table can be seen in Figure 9. In order to have an input de-coupled from the other components (i.e. a vertical force that would not produce also a moment about X or Y) it is important to align the mini-shaker with the axes originated from the center of mass (CoM) of the suspended platform. For the input along Z, the mini-shaker needed to be centered with the top dummy wheel as shown in Figure 9. For input along X or Y, the CoM is placed at a height that is equivalent to the interface plane between the bipods and the top platform. For this reason, the mini-shaker needed to be placed horizontally and attached at the top of the bipod as shown in Figure 10. Three configurations were tested: a case with the coils in open circuit and so no damping (ND), a case in which the coils were connected to the negative resistance converter (WD) and a case with the coils in short-circuit conditions (SC). The last configuration is the equivalent of a particular failure case in which the electronic boards have failed, or lost power and the coils are short-circuited so to continue to work in a completely passive fashion.

The test results for the Z input and X input can be seen in Figure 11 and Figure 12. The comparison with the Simulink model shows good correlation with this complex system at least up to 200Hz. The several peaks that were recorded past that frequency are due to local modes of the dynamometric table and the granite table on top of which it was mounted. In fact, modes at 176, 360, 404, 453, 519, 640 Hz were already recorded before the hexapod was placed on top of the dynamometric table. Further investigation is currently carried out to improve the test setup and reduce the amount of local resonances in the frequency range of interest.

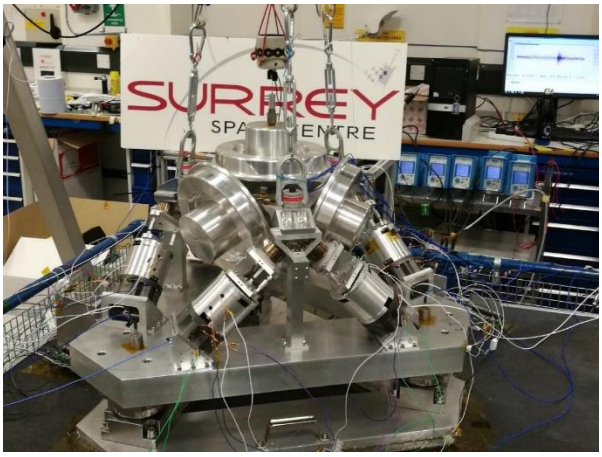

Figure 9. Test setup a hexapod level for the evaluation of the TF33 (i.e. input and output along Z).

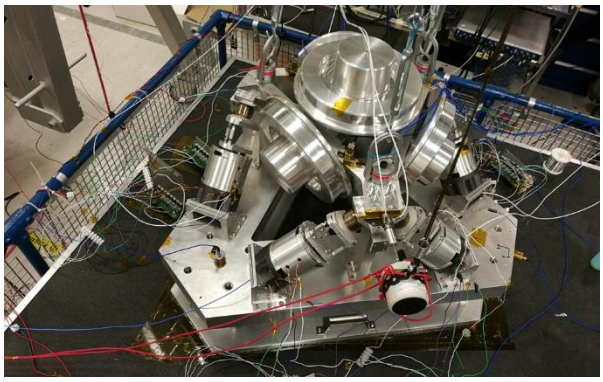

Figure 10. Test setup a hexapod level for the evaluation of the TF11 (i.e. input and output along X).

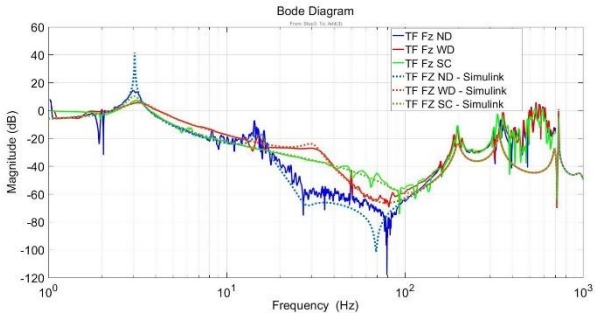

Figure 11. Comparison of TF33 between test results and Simulink simulations. Three cases were tested: without damping (ND), with the EMSD On (WD) and with the electromagnets short-circuited and so without negative resistance circuit (SC)

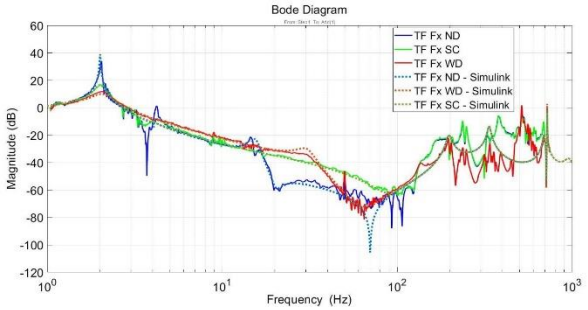

Figure 12. Comparison of TF11 between test results and Simulink simulations. Three cases were tested: without damping (ND), with the EMSD on (WD) and with the electromagnets short-circuited and so without negative resistance circuit (SC)

LESSONS LEARNED

The assembly and testing of the hexapod has been extremely challenging due to the expected high isolation performance. The simulation of the isolation performance was carried out in Simulink, which allows to combine the mechanical and electrical models. However, all the bodies added on a Simulink model are rigid by default and that is often an assumption that is considered too conservative. In reality, the flexibility of the strut parts, especially the ones made in graphite reinforced plastic, affected the frequencies of the secondary bending modes. This effect was observed through a modal analysis in Nastran in which the parts were modelled with the proper material properties. This contraposition between Simulink (used to compute the isolation TFs) and Nastran (to obtain a more accurate modal analysis) needs to be taken into account and it is important to use Nastran as a benchmark and to modify/reduce the stiffnesses in Simulink in order to match the system natural modes.

Another interesting discovery regarded the way the flexure membranes were clamped. Tests at component level on single flexures showed that the flexures had an average of 5e6 N/m of lateral stiffness. However, when the single struts were tested, the bending modes were almost 100Hz lower than the ones originally predicted in Simulink or Nastran. After further investigation, it was concluded that the issue was the way some of the flexures were clamped against graphite parts (with brass inserts used to increase the screw grip in the graphite). This was proven with a more representative test setup at component level, in which a pair of flexure was clamped first against all graphite parts (Figure 13) and then all aluminium parts (Figure 14). Such tests showed that the clamping of the flexure was responsible for a drop of lateral stiffness of more than 50%, and that would be consistent with the bending modes observed a strut level testing.

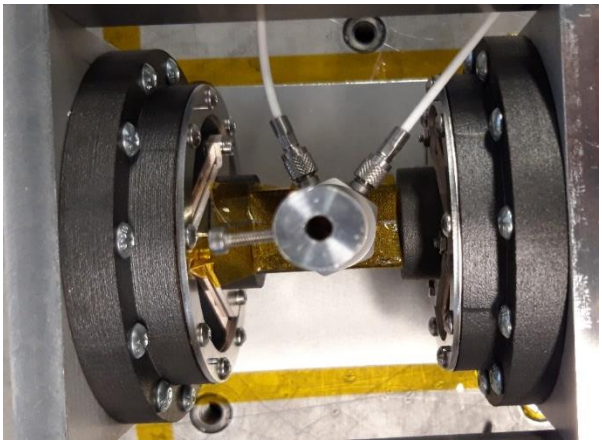

Figure 13: Component test setup to verify lateral stiffness of flexures when clamped against graphite parts

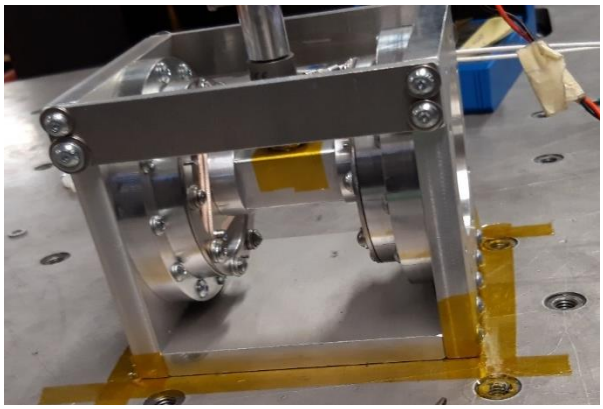

Figure 14: Component test setup to verify lateral stiffness of flexures when clamped against all aluminium parts

In terms of undesired modes recorded above 170Hz, it was mentioned before that those local modes were generated within the dynamometric table and the granite table. Methods have been developed in order to remove some of the local modes during the data post-processing. This was achieved by placing high-sensitive seismic accelerometers on the granite table and on top of the dynamometric table. Through a Nastran model, it has been possible to obtain the mass and inertia involved with the first few local modes and they were applied to the recorded accelerations in order to compensate some of those modes and heavily reduce them in the TFs.

Finally, the offloading of the 30 kg of suspended mass together with the soft nature of the isolation system (first rigid modes all below 5Hz) was also a challenging aspect of the hexapod testing. It was necessary to use bungee cords as other offloading systems (e.g. helium balloons) would not be able to generate the almost 300N of vertical force. The bungee cords needed to have low stiffness so that to not interfere with the hexapod, but that meant also that those cords needed to extend considerably to offload the 30kg. The high-ceiling lab was crucial (3m above the granite table), although a clever disposition of the cords (i.e. combination of series and parallel cords) was needed in order to stay within the maximum height. The cords were supporting the top platform in 3 points, and extendable hooks were used to level the platform within +/- 0.3 deg. During the extensive test campaign, it was observed how the cords, being almost stretched to the limit, were experiencing relaxation/creep and so that corresponded to regularly readjusting their length through the extendable hooks.

CONCLUSIONS

The work presented in this paper is the culmination of more than 2 years of work. Despite this, the technology still requires further development to be ready to fly, the numerous lessons learned and design improvements that were achieved over the last 2 years have pushed this technology considerably further. The many challenges encountered have exposed the difficulty in not only designing but also verifying a high-performance attenuation system like the one presented in this paper. Nevertheless, the good correlation observed with the preliminary test results have demonstrated that this complex system can be simulated with some degree of accuracy and this is a crucial achievement for the next steps. The project team will take into account the lessons learned from this test campaign and will further update the system design. Over the next 2 years, the isolation system will undergo environmental testing and deployment testing so to bring this technology to an engineering model.

ACKNOWLEDGMENTS

The project team would like to thank ESA for the financial support of this project. This work is part of the ESA TRP funding associated with the contract No: 4000125070/18/NL/AR.

REFERENCES

1. Y. Patel and P. George, “Parallel manipulators applications: a survey," Modern Mechanical Engineering, vol. 2, pp. 57 - 64, 2012.
2. B. Dasgupta and T. Mruthyunjaya, “The stewart platform manipulator: a review," Mechanism and Machine Theory, vol. 35, no. 1, pp. 15 - 40, 2000
3. D. Stewart, “A platform with six degrees of freedom," Proceedings of the Institution of Mechanical Engineers, vol. 180, no. 1, pp. 371-386, 1965.
4. V. E. Gough and S. G. Whitehall, “Universal tyre test machine," Proceedings of the FISITA Ninth International Technical Congress, pp. 117-137, 1962.
5. K. L. Cappel, “Motion simulator," US Patent No. 3,295,224, 1967.
6. W. Dongsu and G. Hongbin, “Adaptive sliding control of six-dof flight simulator motion platform," Chinese Journal of Aeronautics, vol. 20, no. 5, pp. 425 - 433, 2007
7. C. Connolly, “Abb highspeed picking robots establish themselves in food packaging," Industrial Robot: An International Journal, vol. 34, no. 4, pp. 281-284, 2007.
8. M. Meggiolaro, S. Dubowsky, and C. Mavroidis, “Error identification and compensation in large

manipulators with application in cancer proton therapy," Sba: Controle Automac~ao Sociedade Brasileira de Automatica, vol. 15, pp. 71 - 77, 03 2004

9. R. G. Cobb, J. M. Sullivan, A. Das, L. P. Davis, T. T. Hyde, T. Davis, Z. H. Rahman, and J. T. Spanos, “Vibration isolation and suppression system for precision payloads in space," Smart Materials and Structures, vol. 8, no. 6, p. 798, 1999
10. E. Anderson, J. Fumo, and R. Erwin, “Satellite ultraquiet isolation technology experiment (suite)," in Aerospace Conference Proceedings, 2000 IEEE, vol. 4, pp. 299-313 vol.4, 2000
11. C. Liu, X. Jing, S. Daley, and F. Li, “Recent advances in micro-vibration isolation," Mechanical Systems and Signal Processing, vol. 56 - 57, pp. 55 - 80, 2015
12. A. Stabile, G. Aglietti, G. Richardson, and G. Smet, “Design and analysis of a novel 2-collinear-dof strut with embedded electromagnetic shunt dampers," Proceedings of ECSSMET, 2016
13. A. Stabile, G. Aglietti, G. Richardson, and G. Smet, “Design and verification of a negative resistance electromagnetic shunt damper for spacecraft micro-vibration," Journal of Sound and Vibration, vol. 386, pp. 38-49, 2017
14. A. Stabile, G. S. Aglietti, G. Richardson, and G. Smet, “A 2-collinear-dof strut with embedded negative-resistance electromagnetic shunt dampers for spacecraft micro-vibration," Smart Materials and Structures, vol. 26, no. 4, p. 045031, 2017
15. A. Stabile, G. Aglietti, G. Richardson, and G. Smet, “Characterization of a novel 2-collinear-DoF strut for Micro-vibration mitigation," Proceedings of ECSSMET, 2018